Atmos. Chem. Phys. Discuss., https://doi.org/10.5194/acp-2018-428
Manuscript under review for journal Atmos. Chem. Phys.
Discussion started: 8 May 2018

Atmospheric Chemistry and Physics Discussions

Characterization of aerosol growth events over Ellesmere Island during summers of 2015 and 2016

Samantha Tremblay[1], Jean-Christophe Picard [1], Jill O. Bachelder[1], Erik Lutsch[2], Kimberly Strong[2], Pierre Fogal[2], W. Richard Leaitch[3], Sangeeta Sharma[3], Felicia Kolonjari[3], Christopher J. Cox[4], Rachel Y.-W. Chang[5], Patrick L. Hayes[1]

[1]Department of Chemistry, Université de Montréal, Montréal, Québec, Canada
[2]Department of Physics, University of Toronto, Toronto, Ontario, Canada
[3]Climate Research Division, Environment and Climate Change Canada, Toronto, Ontario, Canada
[4]Cooperative Institute for Research in Environmental Sciences (CIRES), Boulder, CO, USA and NOAA Physical Sciences Division, Boulder, CO, USA
[5]Department of Physics and Atmospheric Science, Dalhousie University, Halifax, Nova Scotia, Canada

Correspondence to: Patrick L. Hayes (patrick.hayes@umontreal.ca), Rachel Chang (rachel.chang@dal.ca)

Abstract. The occurrence of frequent aerosol nucleation and growth events in the Arctic during summertime may impact the region's climate through increasing the number of cloud condensation nuclei in the Arctic atmosphere. Measurements of aerosol size distributions and aerosol composition were taken during the summers of 2015 and 2016 at Eureka and Alert on Ellesmere Island in Nunavut, Canada. The corresponding results provide a better understanding of the frequency and spatial extent of these nucleation and growth events as well as of the composition and sources of aerosol mass during particle growth. These events are observed beginning in June with the melting of the sea ice rather than with polar sunrise, which strongly suggests emissions from marine sources are the primary cause of the events. Frequent particle nucleation followed by growth occurs throughout the summer. Correlated particle growths events at the two sites, separated by 480 km, indicate conditions existing over such large scales play a key role in determining the timing and the characteristics of the events.

In addition, aerosol mass spectrometry measurements are used to analyze the size-resolved chemical composition of aerosols during two selected growth events. It is found that particles with diameters smaller than 100 nm are predominately organic with only a small sulphate contribution. The oxidation of the organic fraction also changes with particle size with larger particles containing a greater fraction of organic acids relative to other non-acid oxygenates (e.g. alcohols or aldehydes). It is also observed that the relative amount of m/z 44 in the measured mass spectra increases during the growth events suggesting increases in organic acid concentrations in the particle phase.

The nucleation and growth events at Eureka are observed most often when the temperature inversion between the sea and the measurement site (at 610 m ASL) is non-existent or weak allowing presumably fresh marine emissions to be mixed upward to the observatory altitude. While the nature of the gaseous precursors responsible for the growth events are poorly understood, oxidation of dimethyl sulphide alone to produce particle phase sulphate or methanesulphonic acid is not consistent with the measured aerosol composition, suggesting the importance of condensation of other gas phase organic compounds for particle growth.

Atmos. Chem. Phys. Discuss., https://doi.org/10.5194/acp-2018-428
Manuscript under review for journal Atmos. Chem. Phys.
Discussion started: 8 May 2018

Atmospheric Chemistry and Physics Discussions

1 Introduction

Surface aerosol concentrations in the Arctic are characterized by a distinct seasonal cycle, with high mass loadings in the winter followed by very low mass loadings in the summer (Sharma et al. 2004; Quinn et al. 2007; Engvall et al. 2008; Sharma et al. 2013; Tunved et al. 2013; Croft et al. 2016a; Nguyen et al. 2016). This cycle is caused by different transport patterns and by changes in wet deposition, with wintertime air influenced by pollution originating from continental regions at lower latitudes such as Europe, Siberia and even South Asia (Stohl 2006). In contrast, during summertime, air masses originating from lower latitudes experience greater wet deposition during transport northwards, resulting in very few particles arriving to the north. Consequently, local sources dominate the surface aerosol. In wintertime Arctic air near the surface spends about one week continuously above 80°N, whereas in summertime the air near the surface spends about two weeks continuously above 80°N (Stohl 2006), which also increases the relative importance of aerosols originating in the Arctic. The nature and sources of aerosols of Arctic origin during summertime are still poorly understood, although marine and snow or ice-related sources have been suggested in the past (e.g. Fu et al. 2013; Willis et al. 2016). As the Arctic continues to warm and summer sea-ice coverage decreases, contributions from marine sources will likely increase while snow or ice-related sources will decrease. In addition, increased shipping and industrial activities during the Arctic summer in the future could completely shift the relative importance of natural and anthropogenic aerosol sources.

In previous work, aerosol size distribution measurements at Alert and Ny- Ålesund in the Arctic show an annual cycle during which summertime surface aerosols exhibit much smaller particle diameter than wintertime aerosols (Tunved et al. 2013; Croft et al. 2016a). It has been suggested that new particle formation could be the source of these small particles, with dimethyl sulphide (DMS) emitted from the ocean being the key gaseous precursor to less volatile species, such as sulphuric acid and methanesulphonic acid, that contributes to aerosol mass (Chang et al. 2011; Leaitch et al. 2013). Ammonia from sea-bird colonies has also been shown to contribute to new particle formation (Croft et al. 2016b). In tropical marine locations, new particle formation tends to occur in the upper part of the troposphere, usually at the outflow of clouds, and these particles are entrained to the surface through mixing, which contributes to relatively stable aerosol size distributions (Hoppel et al. 1986; Clarke et al. 2006). However, modelling studies of the Arctic summer show that persistent cloud and drizzle causes wet deposition and results in low condensation sinks at the surface. These conditions can favour particle nucleation followed by growth between drizzle events (Browse et al. 2014; Croft et al. 2016a).

Sulphuric acid has long been known to contribute to new particle formation and growth events (Twomey 1977; Charlson et al. 1992; Napari et al. 2002; Lohmann and Feichter 2005; Kirkby et al. 2011; Almeida et al. 2013; Croft et al. 2016b). However, organic compounds, especially those with lower volatilities, are also known to contribute secondary aerosol mass to particle growth and nucleate new particles in forested and anthropogenically influenced regions (Allen et al. 2000; Zhang et al. 2009; Pierce et al. 2012; Riipinen et al. 2012) as well as in laboratory studies (Kirkby et al. 2016; Trostl et al. 2016). Box models have inferred the contribution of non-sulphur species (i.e. organic compounds) to aerosol growth in Greenland (Ziemba et al. 2010) and in tropical marine cloud outflow (Clarke et al. 1998). Burkart et al. (2017) provided

indirect evidence that organic compounds contribute to aerosol growth in high-latitude marine environments using both microphysical modeling of a particle growth event as well as cloud condensation nuclei (CCN) hygroscopicity measurements. Recent work by Mungall et al. (2017) also suggests a marine source of oxygenated volatile organic compounds in the Canadian Arctic, which is photo-mediated and a possible source of precursor vapors for new particle formation or growth.

The GEOS-Chem chemical transport model has been used to model particle formation and size distributions in the Arctic (Bey et al. 2001; Wild and Prather 2006; Croft et al. 2016a; Croft et al. 2016b; Christian et al. 2017). Recent work using GEOS-Chem with the size-resolved aerosol microphysics package TOMAS (Croft et al. 2016a; Croft et al. 2016b) analyzed size distributions of aerosols measured in the Arctic, and showed that GEOS-Chem-TOMAS underestimates Aitken mode particle sizes during the summertime. It was also shown that new particle formation can be driven by neutralization reactions, where missing ammonia emissions can be accounted for by seabird colonies. However, this work acknowledges poor constraints on marine primary aerosol and secondary organic aerosol precursors. These results demonstrate the difficulties that the GEOS-Chem model has in predicting particle size distributions for the Aitken mode during summertime, which is presumably due to missing processes contributing to particle growth (e.g. the condensation of semi-volatile or low-volatility vapors). Similar discrepancies are also observed in the chemical transport model GLOMAP (Global Model of Aerosol Processes) (Korhonen et al. 2008; Browse et al. 2014), with a low bias observed for either Aitken or Accumulation mode aerosols.

In this study we present direct measurements of size-resolved aerosol chemical composition using mass spectrometry to better understand the processes contributing to aerosol growth during the summertime in the Canadian High Arctic. These measurements, as well as those of aerosol number size distribution, were conducted at Eureka, Nunavut on Ellesmere Island in the Canadian Arctic Archipelago. For comparison, aerosol size distributions measured at Alert, which is located further north on Ellesmere Island, are also reported. Numerous concomitant events in which small particles appear and then grow are observed at both sites throughout the summer, resulting in large variations in the number concentration of particles with diameters smaller than 100 nm. The mass spectrometry measurements indicate that these ultrafine particles are predominately organic with a composition that evolves in time during particle growth. Taken together, these results provide important evidence that the condensation of lower volatility organic vapors on particle surfaces leads to frequent particle growth events observed at two sites on Ellesmere Island (e.g. approximately 20 events during summer 2016 at Eureka).

2 Experimental

2.1 Field Site Information and Aerosol Sizing Instrumentation

The primary site at which surface aerosol measurements were taken was the Polar Environment Atmospheric Research Laboratory (PEARL) (Fogal et al. 2013) located on Ellesmere Island in Nunavut, Canada (80.05° N, 86.42° W). The PEARL Ridge Laboratory (RidgeLab) is located 610 m above sea level and 11 km northeast of the Environment and

Climate Change Canada (ECCC) Eureka Weather Station, located at sea level. Radiosondes are launched twice a day from the Weather Station at 00:00 UTC and 12:00 UTC and are used in this work to evaluate the vertical temperature profile and presence of temperature inversions between sea level and the altitude of the RidgeLab. Solar radiation data are measured by a pyranometer (Kipp & Zonen CM 21) at the Surface and Atmospheric Flux, Irradiance and Radiation Extension (SAFIRE) site, situated near Eureka Weather Station at 85 meters above sea level (79.98° N, 85.93° W).

At the PEARL RidgeLab, the instruments sampled year-round through a common aerosol inlet, made of 6 m of stainless steel with a 1 inch outer diameter (OD), sampling 2 m above the roof of the laboratory with a total flow rate of 11 L/min, as previously described by Kuhn et al. (2010). A scanning mobility particle sizer (SMPS, TSI 3034) measured the aerosol size distribution for diameters between 10 and 487 nm in 54 channels, while an optical particle counter (OPC, Met One GT-526S) measured the aerosol size distribution at diameters between 0.3 and 10 μm in six channels. Both instruments are connected to the common inlet. More precisely, the SMPS flow passes first through 0.8 m of 1 inch OD stainless steel tubing connected to the common aerosol inlet; this flow then enters a 3/8 inch OD stainless steel tube with a length of 0.5 m and finally passes through a 1/4 inch OD copper tube that is 1 m long. For the OPC, the flow passes from the common aerosol inlet into a 1/2 inch OD and 0.5 m long copper tube, and then into a 1/4 inch OD and 0.8 m long copper tube, which is connected to the OPC by 1/4 inch OD and 0.04 m long conductive rubber tubing. Particle transmission efficiency to the SMPS has been calculated and the resulting transmission curve is shown in Figure S1 (von der Weiden et al. 2009).

Measurements from these instruments are reported for a period starting in July 2015 through September 2016, and thus consist of one full 2016 summer season and the full summer month of August 2015. (Wintertime measurements are taken too, but are not presented in this article.) Both the OPC and SMPS data are recorded every three minutes, and then subsequently averaged to hourly data for analysis and comparison to other data sets. Agreement between the SMPS and OPC is evaluated by comparing the particle number concentration between 300 – 487 nm measured by the SMPS against the concentration measured by the OPC for approximately the same range of particle diameters (300 – 500 nm). The results are showed in Figure S2 and the agreement is generally satisfactory (slope = 1.3 and 0.96, R^2 = 0.96 and 0.97, for 2015 and 2016 respectively).

The aerosol size distributions measured at the PEARL RidgeLab are compared against those measured at Alert, Nunavut located 480 km to the northeast, where the surface measurements are conducted at the Dr. Neil Trivett Global Atmosphere Watch Observatory (82.5° N, 62.3° W), 210 m above sea level. At this site, particle size distributions between 10 and 487 nm are measured using a SMPS (TSI 3034) (Leaitch et al. 2013).

2.2 Aerosol Mass Spectrometer

Between 26 July and 8 September 2015, a quadrupole aerosol mass spectrometer (AMS, Aerodyne Research Inc.) measured the chemical composition of submicron non-refractory aerosol particles at the PEARL RidgeLab (Canagaratna et al. 2007). Both hourly bulk and size-resolved concentrations were measured by switching between mass spectroscopy (MS) and particle time-of-flight (PToF) modes. All data were analyzed using standard AMS software (AMS Analysis Toolkit

v1.43) with Igor Pro v6.3.7.2 (WaveMetrics). From the common aerosol inlet, the AMS flow passed first through 0.8 m of 1 inch diameter stainless steel tubing and then through a 3/8 inch diameter stainless steel tube with a length of 0.5 m before entering the AMS. The instrument was calibrated multiple times during the measurement period with 300 nm diameter ammonium nitrate particles to determine the ionization efficiency. The aerodynamic diameter was calibrated using polystyrene latex spheres at 80, 125, 240 and 300 nm. Filtered air was sampled every day to establish the air beam corrections. Aerosol mass measured by the AMS was corrected for the instrumental collection efficiency using the method of Middlebrook et al. (2012). The collection efficiency (CE) varied between 0.45 and 0.86 with the increases in CE corresponding to periods when aerosol sulfur was present in its acidic forms (sulphuric acid and ammonium bisulphate) rather than as ammonium sulphate.

To evaluate the accuracy of the AMS measurements, they are compared to PM_1 aerosol concentration determined from the combined SMPS and OPC measurements, as will be discussed later in Section 3. A linear regression analysis of these two quantities resulted in a correlation coefficient of 0.89 and a slope of 1.16. These values confirm that the collection efficiency algorithm from Middlebrook et al. (2012) is reasonable.

2.3 Meteorological Data

Radiosondes (Vaisala RS92-SGP) launched from sea level at the Eureka Weather Station provided different meteorological parameters for altitudes both below and above the PEARL RidgeLab. The radiosondes are launched daily by ECCC meteorological technicians, and the reported data were obtained from the University of Wyoming, Department of Atmospheric Sciences' Upper Air Data Website (http://weather.uwyo.edu/upperair/sounding.html). While the resulting measurements provide a means to evaluate the vertical temperature profile, and thus whether the PEARL RidgeLab at 610 m is located within or above the inversion layer, caution must be taken in interpreting the results due to a number of considerations: (1) the ECCC Weather Station is located approximately 11 km in a straight line from the PEARL RidgeLab, (2) the complex terrain in the region, and (3) the radiosondes do not necessarily fly straight up and can meander significantly after launch because of the wind direction. Therefore, the radiosonde measurements do not necessarily reflect the vertical temperature profile nearer to the PEARL RidgeLab.

2.4 Back-Trajectory Analysis

Air mass histories were computed using the FLEXible PARTicle (FLEXPART (Stohl et al. 2005)) Lagrangian-dispersion model. The tracer particles are inert and non-interacting and are released from the position of the PEARL RidgeLab at an altitude of 610 m above sea level. Backward dispersion runs were initialized by releasing an ensemble of 6000 air-tracer particles over a 6 hour period around the time corresponding to the beginning of a growth event as shown in Table 1. FLEXPART was run in backward mode for 6 days driven by meteorological data from the National Centers for Environmental Prediction (NCEP) Climate Forecast System (CFS V2) 6 hourly product (Saha et al. 2014) to calculate the spatially resolved potential emissions sensitivity (PES), which is proportional to the residence time of a tracer above a given

grid cell. PES represents the amount of time that an air mass is influenced by emissions within a given grid cell during the duration of the FLEXPART run. In this study, the PES is time-integrated over a period of 6 days before the particle release time.

3. Results and Discussion

3.1 Summertime Aerosol Size Distributions

3.1.1 Observations at Eureka and Alert

Figure 1 shows the aerosol size distributions measured at the PEARL RidgeLab and at Alert for 16 June to 26 September 2016. Particle growth events are evident at both sites. Approximately 40 events with elevated concentrations of small particles (< 20 nm diameter) were observed at the PEARL RidgeLab during this period, 22 of which were followed by growth lasting between 2 to 6 days. The sudden appearance of these Aitken mode particles is consistent with previous field observations performed in the Canadian Arctic during research flights and cruises (Chang et al. 2011; Leaitch et al. 2013; Willis et al. 2016; Collins et al. 2017). While the sources of these particles remains poorly understood, this previous work suggested that the formation and growth of ultrafine particles may be due to marine biological activity and the oxidation of DMS and volatile organic compounds (VOCs). The sustained particle growth observed at the PEARL RidgeLab and at Alert, as well as in the previously published work cited above suggests that there is a significant atmospheric reservoir of chemical compounds with volatilities that are low enough to partition to a condensed phase and could thus also be contributing to the nucleation process. Nevertheless, it is not possible to rule out primary marine emissions as a source of particles that provide the necessary surface area for condensing gases (Leck and Bigg 2005). During certain events that exhibit the appearance of Aitken mode particles and subsequent growth, there are also signs of successive events that merge into the growth events from previous days, consistent with other observations in the Arctic (Collins et al. 2017).

Despite being almost 500 km apart, the particle growth events occurred at similar times at both the PEARL RidgeLab and Alert (Figure 1). While simultaneous nucleation events at sites as far apart as 350 km have been observed in continental regions where SO_2 concentrations are high (Jeong et al. 2010; Crippa and Pryor 2013), to our knowledge this work is the first time such a correlation of specific events has been observed in the Arctic, although monthly averages have been previously compared (Freud et al. 2017). It is also important to note substantial topographic barriers exist between the two stations that are located on opposite sides of the Arctic Cordillera, which hinders direct passage of air masses between the two sites (see discussion of back-trajectories in Section 3.1.3). The particle number concentrations measured at the two sites for diameters between 10 and 487 nm are similar for both sites (Figure 2a) and the number concentrations of particles between 20 and 70 nm at the two sites show a moderate correlation with a correlation coefficient of 0.61 (Figure 2b). These results confirm that the growth events have a tendency to occur at similar times at both sites, demonstrating that conditions can exist in the Arctic that are favourable for aerosol growth over distances of at least 500 km, even though mesoscale circulation at the two sites is likely very different (Persson and Stone 2007).

Similar to Figure 1, the aerosol size distributions at the PEARL RidgeLab and Alert were measured for a portion of summer 2015 (26 July to 26 September 2015) as shown in the bottom panels of Figure 3. Again there is a clear association of Aitken mode particles and their subsequent growth at the two sites, leading to the conclusion that the similarities in the growth events at the two sites are not specific to 2016.

In order to evaluate the influence of the appearance of small particles and growth events on the particle number concentrations at the two sites, the total concentration measured by the SMPS is summarized in Figure 4 in a series of box and whisker plots for 2015 and 2016. (Data are only shown for the period of 27 July to 9 September, since measurements at Eureka were unavailable before 27 July 2015.) It is observed that the particle concentrations are similar at the two sites for period studied. For Eureka, the plots indicate a slight increase in the 10^{th}, 25^{th}, 50^{th}, 75^{th} and 90^{th} percentiles in 2016 compared to 2015. In addition, there are similar increases in the particle concentration for Alert when comparing the two years, except for the 90^{th} percentile which is much higher in 2015. During this year, two events with very elevated particle concentration were observed at Alert and coinciding events were observed at Eureka, but at Eureka the particles concentrations were much lower, which explains the higher 90^{th} percentile in 2015 at Alert. The reason for the occurrence of these particular events is unknown. Except for this deviation, the particle number concentrations at the two sites are in general rather similar in both 2015 and 2016. It is important to note that for summer 2016, the mean is approximately 50 – 100 particles cm^{-3} higher than the results shown in Figure 4 if the data for the entire summer of 2016 are used to calculate the percentiles. This observation is explained by the fact that the total duration of the growth events is longer in June and July compared to the months of August and September.

3.1.2 Case Studies of Aerosol Growth Events

To further analyze the growth events and periods with elevated concentrations of ultrafine particles, two different sets of case studies were selected comprising five (Table 1) or 28 events (Table S1). The 28 events represent all the growth events observed during the measurement period, and the smaller set is used to calculate growth rates because the events do not overlap with proceeding or subsequent growth events and exhibit relatively smooth growth curves. For the smaller set of case studies near Eureka, the measured particle size distributions are shown in Figure 5, along with the temperature profiles measured using radiosondes launched from the Eureka Weather Station. The initial growth rates are also included in Table 1 (Kulmala et al. 2004; Hussein et al. 2005; Salma et al. 2011). Looking more closely at the meteorology of the five growth events, one can evaluate the optimal conditions that favor the presence of the growth events at the PEARL RidgeLab. In particular, the absence of an inversion below the PEARL RidgeLab would correspond to air masses measured at the site that are more influenced by local, less photochemically aged and possibly marine sources. In contrast, if the sources of aerosol mass during growth are the sea or the land surface and within the stable stratification, then these influences are expected to be less important when an inversion is present below the PEARL RidgeLab. Figure 5 demonstrates that while temperature inversions that terminate with a maximum below 600 m (the altitude of the PEARL RidgeLab) do sometimes exist before or at the beginning of a growth event, the presence of such inversions is infrequent and often weak (less than 2°C). These

inversion conditions will thus result in air masses measured by the instruments at PEARL that are directly influenced by local emissions near or below the PEARL RidgeLab.

Furthermore, to more systematically analyze the growth events for the summers of 2015 and 2016 at the PEARL RidgeLab, a histogram of the number of events binned by the average inversion temperature (i.e. the temperature at the top of the inversion minus that at the bottom) during each event is plotted in Figure 6. (All the growth events used in creating Figure 6 are summarized in Table S1 and the particle size distributions are shown in Figure S3.) One can see a clear tendency that particle growth events (and presumably nucleation) are more commonly observed when the inversion is weaker or not present. Thus, it can be concluded from Figure 6 that the observation of growth events is more likely when the air at the PEARL RidgeLab is influenced by more recent surface emissions that are likely less photochemically aged. In contrast, when the inversion is strong, the aerosol and aerosol precursor species are more chemically aged due to slower transport into the free troposphere and thus the existing particles have already grown to sizes corresponding to the accumulation mode. A few growth events are observed when the temperature inversion is larger, which may be due to the fact that the radiosondes are launched at the Eureka Weather Station located 11 km to the southwest of the PEARL RidgeLab. Thus, the temperature profile measured by a radiosonde may not be fully representative of that at the RidgeLab. Nevertheless, the observations reported here are consistent with previous work (Willis et al. 2016; Collins et al. 2017) suggesting that similar events measured in the Canadian Arctic are attributable to marine sources.

Many previous studies have characterized aerosol growth rates in remote regions including the Arctic. In particular, Collins et al. (2017) reported growth rates ranging from 0.2 – 15.3 nm h^{-1} during two research cruises conducted in the Canadian Arctic. Using the same analysis method, growth rates ranging from 0.1 – 1.0 nm h^{-1} were determined for the aerosols at the PEARL RidgeLab and at Alert; these values (Table 1) are similar to the range reported in Collins et al. and similar to those reported by Nieminen et al. (2018) for Alert. Furthermore, the growth rates are similar for all the events analyzed in Table 1, with an average and a standard deviation of 0.5 nm hr^{-1} and 0.3 nm hr^{-1}, respectively. This finding suggests that the atmospheric processes (e.g. the condensation of semi-volatile or low volatility vapors to the particle surfaces as discussed below) and conditions governing the growth events are rather consistent in this study.

3.1.3 Back-Trajectory Analysis

To understand the influence of the air mass history on the occurrence of the growth events, back-trajectories were calculated using FLEXPART (Figure S4). This calculation permits the evaluation with precision of the spatial distribution of the potential emissions sensitivity at the beginning of each growth event. In general, these calculations show that the aerosols measured at the PEARL RidgeLab are mostly influenced by source regions located in the Canadian Arctic Archipelago, in Baffin Bay and to the north of Ellesmere Island. However, the analyzed growth events do not have the same air mass history. Five of the growth events are impacted by air from the area of Baffin Bay and the Canadian Arctic Archipelago (GE 3 at Eureka and Alert, GE 6, GE 32, and GE 38). These results mostly coincide with the research reported by Collins et al. (2017), in which they observed high concentrations of ultrafine particles in these regions. On the other hand, for growth

Atmos. Chem. Phys. Discuss., https://doi.org/10.5194/acp-2018-428
Manuscript under review for journal Atmos. Chem. Phys.
Discussion started: 8 May 2018

event 30, which began on 25 June 2016, the FLEXPART calculation indicated a different air mass history compared to the four other growth events. Specifically, the FLEXPART back-trajectory for growth event 30 shows an influence from areas near and further north of Alert, and there is a small contribution from areas in the Nares Strait. Interestingly, NASA WorldView Images (https://worldview.earthdata.nasa.gov/) show that on 25 June 2016 and for several preceding days the ocean in these regions was mostly covered in sea-ice, but there were large areas of open water. In conclusion, growth events can occur within air masses with different back-trajectories, as also reported by Collins et al. (2017), but this work extends this finding to a new domain of the Arctic and to a greater number of growth events. Lastly, by comparing GE 3 at Eureka and at Alert one finds that the growth event has a similar growth rate and a similar back-trajectory at the two sites.

3.2 Aerosol Bulk and Size Resolved Chemical Composition

AMS measurements of aerosol composition and concentration for the summer of 2015 are shown in Figures 3A and 3B, where one sees the mass concentrations for the four dominant types of non-refractory aerosol. During two major growth events in July and August (GE 3 and GE 6), it can be seen that the aerosol organic fraction represents a large majority of the aerosol mass. In contrast, later in the year there is a period of larger particle diameters, and during this period the mass concentration of sulphate is higher than the organic component (approximately 30 August 2015 to 5 September 2015).

While sulphate is a key contributor to nucleation at lower latitudes and is an oxidation product of dimethyl sulphide (DMS) from marine emissions, relatively little sulphate is observed during growth events. At the same time, the observation of relatively high bulk organic aerosol concentrations during Arctic summer is consistent with previous analyses of organic aerosol functional groups in samples collected at Alert (Leaitch et al. 2018). Since the bodies of water in the vicinity of Eureka were relatively open and not covered in sea ice during this period, the water may have been a source of precursors to the observed aerosol mass, which would be consistent with the correlation of the occurrence of growth events and the breakdown of the temperature inversion below the altitude of the PEARL RidgeLab. It is possible that methanesulphonic acid (MSA), an atmospheric oxidation product of DMS, could be contributing to the overall organic mass (Park et al. 2017). However, when the mass spectra for GE 3 and GE 6 are compared against that measured for MSA in the laboratory (Figure S5) (Phinney et al. 2006), it is observed that the ambient spectra are very different from the MSA spectrum. In particular, the relative intensity of m/z 79 is much lower in the ambient spectra. Furthermore, in the MSA spectrum the sulphate fragments at m/z 48 and 64 are much greater than the organic fragments at m/z 43 and 44 whereas these organic fragments have greater intensity in the ambient spectra. Lastly, the correlation coefficient for the two average ambient mass spectra ($R = 0.84$) is much higher than the correlation coefficient between each ambient spectrum and the spectrum measured for MSA ($R = 0.60$ and 0.48 for GE 3 and GE 6 versus MSA, respectively). When taken together, these differences between the ambient and MSA mass spectra indicate that other organics are contributing to the aerosol mass besides MSA.

Following the measurements of the bulk aerosol composition show in Figure 3, the dependence of the composition on the particle size is analyzed in Figure 7. The PToF data reveal that the smallest particles sampled by the AMS (less than 100 nm in diameter) during the two different growth events were enriched in organics, with little to no sulphate. Above 100

nm, the measured aerosol composition changes depending on the particles size and the larger aerosol particles contain a greater fraction of sulphate.

To further evaluate the organic aerosol composition only, two important fragments in the measured mass spectra of the organic aerosol, m/z 43 and 44, are plotted in Figure 7e and Figure 7f. For the organic aerosol, m/z 44 corresponds to the concentration of carboxylic acids, whereas m/z 43 correlates with other oxygen containing functional groups in the particle phase (e.g. alcohols). The size-resolved measurements of these fragments show that the organic composition varies with particle size. The smallest particles are less oxidized, with the fraction of carboxylic acids increasing with the particle diameter between 100 and 500 nm. While this relative trend is observed for both growth events, the absolute ratios of m/z 43 to m/z 44 are not the same, which indicates some variation in the amount oxidation of the organic aerosol during growth events. Overall, the size-resolved measurements indicate that for the two growth events analyzed here, which occurred during summer 2015, the mass of the growing particles is predominately organic matter.

To complement the analysis of the organic aerosol composition shown in Figure 7, the fractions of the total organic mass measured at m/z 43 and at m/z 44 (abbreviated as f_{43} and f_{44}) are plotted against each other in Figure 8, in which the data are colored as a function of time. Lambe et al. (2011) demonstrated in a series of lab studies that secondary organic aerosol (SOA) formed from a variety of different precursors, both anthropogenic and biogenic, falls within a well-defined space in the f_{44} versus f_{43} plot, which is shown as the black triangle in Figure 8. The organic aerosols measured at the PEARL RidgeLab have f_{44} and f_{43} ratios that are consistent with the previous work of Lambe et al. and others (Ng et al. 2011). Furthermore, the f_{44} and f_{43} values for the seven hours at the beginning or at the end of each growth event were averaged and plotted in Figure 8 in order to evaluate the overall change in SOA composition. For GE 3, there is a clear trend during the evolution of the growth event wherein both f_{44} and f_{43} increase, which is consistent with an increase in the relative concentration of carboxylic acids and non-acid oxygenates in the organic aerosol. For GE 6, the change in composition is less evident. The value of f_{44} increases, but f_{43} decreases, and in addition the trend with time is not as clear as for GE 3. A possible explanation for the decrease in f_{43} during GE 6 is a decrease in the $C_3H_7^+$ fragment, which originates from alkyl groups in the organic aerosol. Regardless, one can conclude that the aerosol growth events coincide with an increase in the amount of oxidation of the organic aerosol likely due to, in part, the production of carboxylic acids. This finding is consistent with the size-resolved composition measurements shown in Figure 7, where smaller particles have a higher fraction of m/z 43 and larger particles formed later during the growth events have a higher fraction of m/z 44.

In summary, the concentration and evolution of oxygenated organics as well as the presence of small organic particles measured by the AMS together suggest that SOA formation contributes to particle growth measured at the PEARL RidgeLab. While the origin of the SOA precursors is not known, it can be concluded that the organic composition is not consistent with SOA formation from MSA alone. Recently published work has suggested that marine microbial processes may be an important source of these VOCs (Collins et al. 2017). Abiotic heterogeneous processes in the marine boundary layer may also be a source of oxidized VOCs as indicated in several laboratory studies (Bruggemann et al. 2017; Chiu et al. 2017). Consistent with this previous research, the first growth event observed at the PEARL RidgeLab in 2016, coincided

approximately with the melting of the sea ice in the Slidre Fjord and the Eureka Sound located to the south and west of the PEARL RidgeLab. Observations of the sea ice taken from the PEARL RidgeLab are shown in the Supporting Information (Figure S6). The pictures show, for summer 2016, the sea ice during the first (25 June 2016) and last (10 September 2016) growth events. Also shown are two additional images. One is of the first time that open water is observed (14 July 2016), and the other is the last available image of the sea ice for 2016 (28 September 2016). On 25 June, it is not possible to see regions of open water during the first growth event. However, open water is observed 300 km to the south of Eureka on the same day in NASA worldview images (https://worldview.earthdata.nasa.gov/). Moreover, the NASA worldview images show open water on 7 July in Eureka Sound and Slidre Fjord. It should also be noted that the first growth event occurred much later than the polar sunrise, which was approximately 21 February 2016. During the last observed growth event (10 September 2016) there is very little or no sea ice, and open water is observed to be persistent until the end of September. This is consistent with measurements of DMS and MSA at Alert which show relatively high concentrations persisting into September (Sharma et al. 2012; Leaitch et al. 2013). Given these observations, there is a possible relationship between the onset of the growth events and the melting of the sea ice in the region around Eureka. This observation is consistent with back-trajectory analyses showing that newly formed particles measured during summertime cruises in the Arctic Ocean are associated with air that has experienced more open water or melting sea ice regions (Heintzenberg et al. 2015; Dall'Osto et al. 2017). Whereas, the decrease in the number of events in September is more likely due to the lack of solar radiation as shown in Figure S7 or measured previously at Alert (Sharma et al. 2012), which limits photochemistry. This finding supports the recent suggestion that photochemical processing of emissions from the ocean may be a source of ultrafine particles in the Arctic (Collins et al. 2017).

4. Conclusions

In this study, new particle growth events were characterized during the summers of 2015 and 2016 at the PEARL RidgeLab (in Eureka, Nunavut, Canada) as well as at Alert, Canada. Both sites are located on Ellesmere Island separated by a distance of 480 km providing an opportunity to evaluate the growth events on a regional scale for the complete 2016 summer season as well as for a portion of the 2015 summer season. During both years, frequent growth events occurred and these events were correlated between the sites. In addition to the concomitant events, the particle concentrations measured at Alert and the PEARL RidgeLab were similar, with the 10^{th}, 25^{th}, 50^{th}, 75^{th} and 90^{th} percentiles not varying by more than a factor of 1.67 suggesting the growth events are not isolated local events. Additionally, the analysis of the growth rates from a subset of events at the PEARL RidgeLab and Alert gives an average rate of particle growth of 0.5(±0.3) nm hr^{-1}. In total, the measurements of the particle number size distribution support the conclusion that particle nucleation and growth events can occur over spatial scales of at least 500 km in the Canadian Arctic Archipelago.

Moreover, in this study AMS measurements showed that particles smaller than 100 nm in diameter are predominately organic with the organic-to-sulphate ratio increasing for smaller particle sizes. This result is in contrast to previous indirect measurements of aerosol composition using a volatility tandem differential mobility analyzer system

installed near Ny-Ålesund, Svalbard (Giamarelou et al. 2016), which suggested that the Aitken mode particles were predominately ammonium sulphate, although it was not possible in that study to conclusively distinguish ammonium sulphate from organics with similar volatility. The amount of oxidation of the organic fraction also changes with particle size, with the ratio of m/z 43 to m/z 44 increasing for smaller particles sizes, which is consistent with a greater fraction of non-acid oxygenates relative to carboxylic acids. The relative concentrations of oxygenated organics were also analyzed in plots of f_{44} against f_{43}, and it was observed that the oxidation of the organic aerosol mass tends to increase during the growth events. Overall, the AMS measurements support the conclusion that condensation of organic vapors contributes to particle growth.

It has been recently suggested that secondary organic aerosols formed from VOCs emitted by marine sources may be an important source of ultrafine particles in the Arctic during summertime. The results of the research presented here are consistent with this possibility. In addition to the SMPS and AMS measurements discussed above, when comparing the growth events against the inversion layer height and temperature change, the growth events are most likely to reach the PEARL RidgeLab when the inversion is non-existent or weak allowing the site's instruments to sample the boundary layer which presumably contains fresh marine emissions. In addition, the onset of the growth events approximately coincides with the opening of the sea ice near the PEARL RidgeLab, rather than polar sunrise. However, future work should focus on the incorporation of more sea ice data as well as further gas phase measurements to understand the timing and chemical processes driving particle nucleation and growth.

Acknowledgements

This work was partially supported by the Université de Montréal and the Natural Science and Engineering Research Council of Canada (Discovery Grant RGPIN-05002-2014, Discovery Grant RGPIN-05173-2014 and Climate Change and Atmospheric Research (CCAR) Program funding awarded to the Probing the Atmosphere of the High Arctic (PAHA) project led by PI James R. Drummond). Support from Environment and Climate Change Canada (ECCC) for the Arctic field work performed at both Eureka and Alert is also acknowledged. The co-authors also acknowledge Canadian Forces Station Alert for the maintenance of Alert base. The authors also acknowledge the use of the FLEXPART Lagrangian dispersion model (https://www. flexpart.eu/wiki/FpDownloads) and the use of the Pflexible Python module (https://bitbucket.org/jfburkhart/pflexible) developed by John F. Burkhart, which was modified here to plot the FLEXPART sensitivities in this paper. The NCEP CFS data used are listed in the references. Radiation measurements have received support from ECCC, CANDAC and the Arctic Research Program of the NOAA Climate Program Office.

Atmos. Chem. Phys. Discuss., https://doi.org/10.5194/acp-2018-428
Manuscript under review for journal Atmos. Chem. Phys.
Discussion started: 8 May 2018

Atmospheric Chemistry and Physics Discussions

References

Allen, M. R., Stott, P. A., Mitchell, J. F. B., Schnur, R., and Delworth, T. L.: Quantifying the uncertainty in forecasts of anthropogenic climate change, Nature, 407, 617-620, 2000.

Almeida, J., Schobesberger, S., Kurten, A., Ortega, I. K., Kupiainen-Maatta, O., Praplan, A. P., Adamov, A., Amorim, A., Bianchi, F., Breitenlechner, M., David, A., Dommen, J., Donahue, N. M., Downard, A., Dunne, E., Duplissy, J., Ehrhart, S., Flagan, R. C., Franchin, A., Guida, R., Hakala, J., Hansel, A., Heinritzi, M., Henschel, H., Jokinen, T., Junninen, H., Kajos, M., Kangasluoma, J., Keskinen, H., Kupc, A., Kurten, T., Kvashin, A. N., Laaksonen, A., Lehtipalo, K., Leiminger, M., Leppa, J., Loukonen, V., Makhmutov, V., Mathot, S., McGrath, M. J., Nieminen, T., Olenius, T., Onnela, A., Petaja, T., Riccobono, F., Riipinen, I., Rissanen, M., Rondo, L., Ruuskanen, T., Santos, F. D., Sarnela, N., Schallhart, S., Schnitzhofer, R., Seinfeld, J. H., Simon, M., Sipila, M., Stozhkov, Y., Stratmann, F., Tome, A., Trostl, J., Tsagkogeorgas, G., Vaattovaara, P., Viisanen, Y., Virtanen, A., Vrtala, A., Wagner, P. E., Weingartner, E., Wex, H., Williamson, C., Wimmer, D., Ye, P. L., Yli-Juuti, T., Carslaw, K. S., Kulmala, M., Curtius, J., Baltensperger, U., Worsnop, D. R., Vehkamaki, H., and Kirkby, J.: Molecular understanding of sulphuric acid-amine particle nucleation in the atmosphere, Nature, 502, 359-369, 2013.

Bey, I., Jacob, D. J., Yantosca, R. M., Logan, J. A., Field, B. D., Fiore, A. M., Li, Q. B., Liu, H. G. Y., Mickley, L. J., and Schultz, M. G.: Global modeling of tropospheric chemistry with assimilated meteorology: Model description and evaluation, Journal of Geophysical Research-Atmospheres, 106, 23073-23095, 2001.

Browse, J., Carslaw, K. S., Mann, G. W., Birch, C. E., Arnold, S. R., and Leck, C.: The complex response of Arctic aerosol to sea-ice retreat, Atmospheric Chemistry and Physics, 14, 7543-7557, 2014.

Bruggemann, M., Hayeck, N., Bonnineau, C., Pesce, S., Alpert, P. A., Perrier, S., Zuth, C., Hoffmann, T., Chen, J. M., and George, C.: Interfacial photochemistry of biogenic surfactants: a major source of abiotic volatile organic compounds, Faraday Discussions, 200, 59-74, 2017.

Burkart, J., Hodshire, A. L., Mungall, E. L., Pierce J., R., Collins, D. B., Ladino, L. A., Lee, A. K. Y., Irish, V., Wentzell, J. J. B., Liggio, J., Papakyriakou, T., Murphy, J., and Abbatt, J.: Organic Condensation and Particle Growth to CCN Sizes in the Summertime Marine Arctic Is Driven by Materials More Semivolatile Than at Continental Sites, Geophysical Research Letters, 44, 10725-10734, 2017.

Canagaratna, M. R., Jayne, J. T., Jimenez, J. L., Allan, J. D., Alfarra, M. R., Zhang, Q., Onasch, T. B., Drewnick, F., Coe, H., Middlebrook, A., Delia, A., Williams, L. R., Trimborn, A. M., Northway, M. J., DeCarlo, P. F., Kolb, C. E., Davidovits, P., and Worsnop, D. R.: Chemical and microphysical characterization of ambient aerosols with the aerodyne aerosol mass spectrometer, Mass Spectrometry Reviews, 26, 185-222, 2007.

Chang, R. Y. W., Sjostedt, S. J., Pierce, J. R., Papakyriakou, T. N., Scarratt, M. G., Michaud, S., Levasseur, M., Leaitch, W. R., and Abbatt, J. P. D.: Relating atmospheric and oceanic DMS levels to particle nucleation events in the Canadian Arctic, Journal of Geophysical Research-Atmospheres, 116, D00s03, 2011.

Charlson, R. J., Schwartz, S. E., Hales, J. M., Cess, R. D., Coakley, J. A., Hansen, J. E., and Hofmann, D. J.: Climate forcing by anthropogenic aerosols, Science, 255, 423-430, 1992.

Chiu, R., Tinel, L., Gonzalez, L., Ciuraru, R., Bernard, F., George, C., and Volkamer, R.: UV photochemistry of carboxylic acids at the air-sea boundary: A relevant source of glyoxal and other oxygenated VOC in the marine atmosphere, Geophysical Research Letters, 44, 1079-1087, 2017.

Christian, K. E., Brune, W. H., and Mao, J. Q.: Global sensitivity analysis of the GEOS-Chem chemical transport model: ozone and hydrogen oxides during ARCTAS (2008), Atmospheric Chemistry and Physics, 17, 3769-3784, 2017.

Clarke, A. D., Davis, D., Kapustin, V. N., Eisele, F., Chen, G., Paluch, I., Lenschow, D., Bandy, A. R., Thornton, D., Moore, K., Mauldin, L., Tanner, D., Litchy, M., Carroll, M. A., Collins, J., and Albercook, C.: Particle nucleation in the tropical boundary layer and its coupling to marine sulfur sources, Science, 282, 89-92, 1998.

Clarke, A. D., Owens, S. R., and Zhou, J. C.: An ultrafine sea-salt flux from breaking waves: Implications for cloud condensation nuclei in the remote marine atmosphere, Journal of Geophysical Research-Atmospheres, 111, D06202, 2006.

Collins, D. B., Burkart, J., Chang, R. Y. W., Lizotte, M., Boivin-Rioux, A., Blais, M., Mungall, E. L., Boyer, M., Irish, V. E., Massé, G., Kunkel, D., Tremblay, J. É, Papakyriakou, T., Bertram, A. K., Bozem, H., Gosselin, M., Levasseur, M., and Abbatt, J. P. D.: Frequent Ultrafine Particle Formation and growth in the Canadian Arctic marine and coastal environment, Atmospheric Chemistry and Physics, 17, 13119-13138, 2017.

Crippa, P., and Pryor, S. C.: Spatial and temporal scales of new particle formation events in eastern North America, Atmospheric Environment, 75, 257-264, 2013.

Croft, B., Martin, R. V., Leaitch, W. R., Tunved, P., Breider, T. J., D'Andrea, S. D., and Pierce, J. R.: Processes controlling the annual cycle of Arctic aerosol number and size distributions, Atmospheric Chemistry and Physics, 16, 3665-3682, 2016a.

Croft, B., Wentworth, G. R., Martin, R. V., Leaitch, W. R., Murphy, J. G., Murphy, B. N., Kodros, J. K., Abbatt, J. P. D., and Pierce, J. R.: Contribution of Arctic seabird-colony ammonia to atmospheric particles and cloud-albedo radiative effect, Nature Communications, 7, 13444, 2016b.

Dall'Osto, M., Beddows, D. C. S., Tunved, P., Krejci, R., Strom, J., Hansson, H. C., Yoon, Y. J., Park, K. T., Becagli, S., Udisti, R., Onasch, T., O'Dowd, C. D., Simo, R., and Harrison, R. M.: Arctic sea ice melt leads to atmospheric new particle formation, Scientific Reports, 7, 2017.

Engvall, A. C., Krejci, R., Strom, J., Treffeisen, R., Scheele, R., Hermansen, O., and Paatero, J.: Changes in aerosol properties during spring-summer period in the Arctic troposphere, Atmospheric Chemistry and Physics, 8, 445-462, 2008.

Fogal, P. F., LeBlanc, L. M., and Drummond, J. R.: The Polar Environment Atmospheric Research Laboratory (PEARL): Sounding the Atmosphere at 80 degrees North, Arctic, 66, 377-386, 2013.

Freud, E., Krejci, R., Tunved, P., Leaitch, R., Nguyen, Q. T., Massling, A., Skov, H., and Barrie, L.: Pan-Arctic aerosol number size distributions: seasonality and transport patterns, Atmospheric Chemistry and Physics, 17, 8101-8128, 2017.

Fu, P. Q., Kawamura, K., Chen, J., Charriere, B., and Sempere, R.: Organic molecular composition of marine aerosols over the Arctic Ocean in summer: contributions of primary emission and secondary aerosol formation, Biogeosciences, 10, 653-667, 2013.

Giamarelou, M., Eleftheriadis, K., Nyeki, S., Tunved, P., Torseth, K., and Biskos, G.: Indirect evidence of the composition of nucleation mode atmospheric particles in the high Arctic, Journal of Geophysical Research-Atmospheres, 121, 965-975, 2016.

Heintzenberg, J., Leck, C., and Tunved, P.: Potential source regions and processes of aerosol in the summer Arctic, Atmospheric Chemistry and Physics, 15, 6487-6502, 2015.

Hoppel, W. A., Frick, G. M., and Larson, R. E.: Effect of nonprecipitating clouds on the aerosol size distribution in the marine boundary-layer, Geophysical Research Letters, 13, 125-128, 1986.

Hussein, T., Dal Maso, M., Petaja, T., Koponen, I. K., Paatero, P., Aalto, P. P., Hameri, K., and Kulmala, M.: Evaluation of an automatic algorithm for fitting the particle number size distributions, Boreal Environment Research, 10, 337-355, 2005.

Jeong, C. H., Evans, G. J., McGuire, M. L., Chang, R. Y. W., Abbatt, J. P. D., Zeromskiene, K., Mozurkewich, M., Li, S. M., and Leaitch, A. R.: Particle formation and growth at five rural and urban sites, Atmospheric Chemistry and Physics, 10, 7979-7995, 2010.

Kirkby, J., Curtius, J., Almeida, J., Dunne, E., Duplissy, J., Ehrhart, S., Franchin, A., Gagne, S., Ickes, L., Kurten, A., Kupc, A., Metzger, A., Riccobono, F., Rondo, L., Schobesberger, S., Tsagkogeorgas, G., Wimmer, D., Amorim, A., Bianchi, F., Breitenlechner, M., David, A., Dommen, J., Downard, A., Ehn, M., Flagan, R. C., Haider, S., Hansel, A., Hauser, D., Jud, W., Junninen, H., Kreissl, F., Kvashin, A., Laaksonen, A., Lehtipalo, K., Lima, J., Lovejoy, E. R., Makhmutov, V., Mathot, S., Mikkila, J., Minginette, P., Mogo, S., Nieminen, T., Onnela, A., Pereira, P., Petaja, T., Schnitzhofer, R., Seinfeld, J. H., Sipila, M., Stozhkov, Y., Stratmann, F., Tome, A., Vanhanen, J., Viisanen, Y., Vrtala, A., Wagner, P. E., Walther, H., Weingartner, E., Wex, H., Winkler, P. M., Carslaw, K. S., Worsnop, D. R., Baltensperger, U., and Kulmala, M.: Role of sulphuric acid, ammonia and galactic cosmic rays in atmospheric aerosol nucleation, Nature, 476, 429-U477, 2011.

Kirkby, J., Duplissy, J., Sengupta, K., Frege, C., Gordon, H., Williamson, C., Heinritzi, M., Simon, M., Yan, C., Almeida, J., Trostl, J., Nieminen, T., Ortega, I. K., Wagner, R., Adamov, A., Amorim, A., Bernhammer, A. K., Bianchi, F., Breitenlechner, M., Brilke, S., Chen, X. M., Craven, J., Dias, A., Ehrhart, S., Flagan, R. C., Franchin, A., Fuchs, C., Guida, R., Hakala, J., Hoyle, C. R., Jokinen, T., Junninen, H., Kangasluoma, J., Kim, J., Krapf, M., Kurten, A., Laaksonen, A., Lehtipalo, K., Makhmutov, V., Mathot, S., Molteni, U., Onnela, A., Perakyla, O., Piel, F., Petaja, T., Praplan, A. P., Pringle, K., Rap, A., Richards, N. A. D., Riipinen, I., Rissanen, M. P., Rondo, L., Sarnela, N., Schobesberger, S., Scott, C. E., Seinfeld, J. H., Sipila, M., Steiner, G., Stozhkov, Y., Stratmann, F., Tome, A., Virtanen, A., Vogel, A. L., Wagner, A. C., Wagner, P. E., Weingartner, E., Wimmer, D., Winkler, P. M., Ye, P. L., Zhang, X., Hansel, A., Dommen, J., Donahue, N. M., Worsnop, D. R., Baltensperger, U., Kulmala, M., Carslaw, K. S., and Curtius, J.: Ion-induced nucleation of pure biogenic particles, Nature, 533, 521-526, 2016.

Korhonen, H., Carslaw, K. S., Spracklen, D. V., Ridley, D. A., and Strom, J.: A global model study of processes controlling aerosol size distributions in the Arctic spring and summer, Journal of Geophysical Research-Atmospheres, 113, D08211, 2008.

Kuhn, T., Damoah, R., Bacak, A., and Sloan, J. J.: Characterising aerosol transport into the Canadian High Arctic using aerosol mass spectrometry and Lagrangian modelling, Atmospheric Chemistry and Physics, 10, 10489-10502, 2010.

Kulmala, M., Vehkamaki, H., Petaja, T., Dal Maso, M., Lauri, A., Kerminen, V. M., Birmili, W., and McMurry, P. H.: Formation and growth rates of ultrafine atmospheric particles: a review of observations, Journal of Aerosol Science, 35, 143-176, 2004.

Lambe, A. T., Onasch, T. B., Massoli, P., Croasdale, D. R., Wright, J. P., Ahern, A. T., Williams, L. R., Worsnop, D. R., Brune, W. H., and Davidovits, P.: Laboratory studies of the chemical composition and cloud condensation nuclei (CCN) activity of secondary organic aerosol (SOA) and oxidized primary organic aerosol (OPOA), Atmospheric Chemistry and Physics, 11, 8913-8928, 2011.

Leaitch, W. R., Russell, L. M., Liu, J., Kolonjari, F., Toom, D., Huang, L., Sharma, S., Chivulescu, A., Veber, D., and Zhang, W.: Organic Functional Groups in the Submicron Aerosol at 82.5° N from 2012 to 2014, Atmospheric Chemistry and Physics, 18, 3269-3287, 2018.

Leaitch, W. R., Sharma, S., L., Huang, Toom-Sauntry, D., Chivulescu, A., Macdonald, A. M., von Salzen, K., Pierce J., R., Bertram, A. K., Schroder, J. C., Shantz, N. C., Chang, R. Y.-W., and A.-L., Norman: Dimethyl sulfide control of the clean summertime Arctic aerosol and cloud. Elem Sci Anth., Elementa Science of the Antropocene, 1, 17, 2013.

Leck, C., and Bigg, E. K.: Biogenic particles in the surface microlayer and overlaying atmosphere in the central Arctic Ocean during summer, Tellus Series B-Chemical and Physical Meteorology, 57, 305-316, 2005.

Lohmann, U., and Feichter, J.: Global indirect aerosol effects: a review, Atmospheric Chemistry and Physics, 5, 715-737, 2005.

Middlebrook, A. M., Bahreini, R., Jimenez, J. L., and Canagaratna, M. R.: Evaluation of Composition-Dependent Collection Efficiencies for the Aerodyne Aerosol Mass Spectrometer using Field Data, Aerosol Science and Technology, 46, 258-271, 2012.

Mungall, E. L., Abbatt, J. P. D., Wentzell, J. J. B., Lee, A. K. Y., Thomas, J. L., Blais, M., Gosselin, M., Miller, L. A., Papakyriakou, T., Willis, M. D., and Liggio, J.: Microlayer source of oxygenated volatile organic compounds in the summertime marine Arctic boundary layer, Proceedings of the National Academy of Sciences of the United States of America, 114, 6203-6208, 2017.

Napari, I., Noppel, M., Vehkamaki, H., and Kulmala, M.: Parametrization of ternary nucleation rates for H(2)SO(4)-NH(3)-H(2)O vapors, Journal of Geophysical Research-Atmospheres, 107, 4381, 2002.

Ng, N. L., Canagaratna, M. R., Jimenez, J. L., Chhabra, P. S., Seinfeld, J. H., and Worsnop, D. R.: Changes in organic aerosol composition with aging inferred from aerosol mass spectra, Atmospheric Chemistry and Physics, 11, 6465-6474, 2011.

Nguyen, Q. T., Glasius, M., Sorensen, L. L., Jensen, B., Skov, H., Birmili, W., Wiedensohler, A., Kristensson, A., Nojgaard, J. K., and Massling, A.: Seasonal variation of atmospheric particle number concentrations, new particle formation and atmospheric oxidation capacity at the high Arctic site Villum Research Station, Station Nord, Atmospheric Chemistry and Physics, 16, 11319-11336, 2016.

Nieminen, T., Kerminen, V. M., Petäjä, T., Aalto, P. P., Arshinov, M., Asmi, E., Baltensperger, U., Beddows, D. C. S., Beukes, J. P., Collins, D., Ding, A., Harrison, R. M., Henzing, B., Hooda, R., Hu, M., Hõrrak, U., Kivekäs, N., Komsaare, K., Krejci, R., Kristensson, A., Laakso, L., Laaksonen, A., Leaitch, W. R., Lihavainen, H., Mihalopoulos, N., Németh, Z., Nie, W., O'Dowd, C., Salma, I., Sellegri, K., Svenningsson, B., Swietlicki, E., Tunved, P., Ulevicius, V., Vakkari, V., Vana, M., Wiedensohler, A., Wu, Z., Virtanen, A., and Kulmala, M.: Global analysis of continental boundary layer new particle formation based on long-term measurements, Atmospheric Chemistry and Physics Discussion, 2018, 1-34, 2018.

Park, K. T., Jang, S., Lee, K., Yoon, Y. J., Kim, M. S., Park, K., Cho, H. J., Kang, J. H., Udisti, R., Lee, B. Y., and Shin, K. H.: Observational evidence for the formation of DMS-derived aerosols during Arctic phytoplankton blooms, Atmospheric Chemistry and Physics, 17, 9665-9675, 2017.

Persson, P. Ola G., and Stone, R.: Evidence of forcing of Arctic regional climates by mesoscale processes, AMS Symposium on Connections between Mesoscale Processes and Climate Variability, 2007. https://ams.confex.com/ams/pdfpapers/119015.pdf.

Phinney, L., Leaitch, W. R., Lohmann, U., Boudries, H., Worsnop, D. R., Jayne, J. T., Toom-Sauntry, D., Wadleigh, M., Sharma, S., and Shantz, N.: Characterization of the aerosol over the sub-arctic north east Pacific Ocean, Deep-Sea Research Part II - Topical Studies in Oceanography, 53, 2410-2433, 2006.

Pierce, J. R., Leaitch, W. R., Liggio, J., Westervelt, D. M., Wainwright, C. D., Abbatt, J. P. D., Ahlm, L., Al-Basheer, W., Cziczo, D. J., Hayden, K. L., Lee, A. K. Y., Li, S. M., Russell, L. M., Sjostedt, S. J., Strawbridge, K. B., Travis, M., Vlasenko, A., Wentzell, J. J. B., Wiebe, H. A., Wong, J. P. S., and Macdonald, A. M.: Nucleation and condensational growth to CCN sizes during a sustained pristine biogenic SOA event in a forested mountain valley, Atmospheric Chemistry and Physics, 12, 3147-3163, 2012.

Quinn, P. K., Shaw, G., Andrews, E., Dutton, E. G., Ruoho-Airola, T., and Gong, S. L.: Arctic haze: current trends and knowledge gaps, Tellus Series B-Chemical and Physical Meteorology, 59, 99-114, 2007.

Riipinen, I., Yli-Juuti, T., Pierce, J. R., Petaja, T., Worsnop, D. R., Kulmala, M., and Donahue, N. M.: The contribution of organics to atmospheric nanoparticle growth, Nature Geoscience, 5, 453-458, 2012.

Saha, Suranjana, Moorthi, Shrinivas, Wu, Xingren, Wang, Jiande, Nadiga, Sudhir, Tripp, Patrick, Behringer, David, Hou, Yu-Tai, Chuang, Hui-ya, Iredell, Mark, Ek, Michael, Meng, Jesse, Yang, Rongqian, Mendez, Malaquias Pena, Dool, Huug van den, Zhang, Qin,

Wang, Wanqiu, Chen, Mingyue, and Becker, Emily: The NCEP Climate Forecast System Version 2, Journal of Climate, 27, 2185-2208, 2014.

Salma, I., Borsos, T., Weidinger, T., Aalto, P., Hussein, T., Dal Maso, M., and Kulmala, M.: Production, growth and properties of ultrafine atmospheric aerosol particles in an urban environment, Atmospheric Chemistry and Physics, 11, 1339-1353, 2011.

Sharma, S., Chan, E., Ishizawa, M., Toom-Sauntry, D., Gong, S. L., Li, S. M., Tarasick, D. W., Leaitch, W. R., Norman, A., Quinn, P. K., Bates, T. S., Levasseur, M., Barrie, L. A., and Maenhaut, W.: Influence of transport and ocean ice extent on biogenic aerosol sulfur in the Arctic atmosphere, Journal of Geophysical Research-Atmospheres, 117, D12209, 2012.

Sharma, S., Ishizawa, M., Chan, D., Lavoue, D., Andrews, E., Eleftheriadis, K., and Maksyutov, S.: 16-year simulation of Arctic black carbon: Transport, source contribution, and sensitivity analysis on deposition, Journal of Geophysical Research-Atmospheres, 118, 943-964, 2013.

Sharma, S., Lavoue, D., Cachier, H., Barrie, L. A., and Gong, S. L.: Long-term trends of the black carbon concentrations in the Canadian Arctic, Journal of Geophysical Research-Atmospheres, 109, D15203, 2004.

Stohl, A.: Characteristics of atmospheric transport into the Arctic troposphere, Journal of Geophysical Research-Atmospheres, 111, D11306, 2006.

Stohl, A., Forster, C., Frank, A., Seibert, P., and Wotawa, G.: Technical note: The Lagrangian particle dispersion model FLEXPART version 6.2, Atmospheric Chemistry and Physics, 5, 2461-2474, 2005.

Trostl, J., Chuang, W. K., Gordon, H., Heinritzi, M., Yan, C., Molteni, U., Ahlm, L., Frege, C., Bianchi, F., Wagner, R., Simon, M., Lehtipalo, K., Williamson, C., Craven, J. S., Duplissy, J., Adamov, A., Almeida, J., Bernhammer, A. K., Breitenlechner, M., Brilke, S., Dias, A., Ehrhart, S., Flagan, R. C., Franchin, A., Fuchs, C., Guida, R., Gysel, M., Hansel, A., Hoyle, C. R., Jokinen, T., Junninen, H., Kangasluoma, J., Keskinen, H., Kim, J., Krapf, M., Kurten, A., Laaksonen, A., Lawler, M., Leiminger, M., Mathot, S., Mohler, O., Nieminen, T., Onnela, A., Petaja, T., Piel, F. M., Miettinen, P., Rissanen, M. P., Rondo, L., Sarnela, N., Schobesberger, S., Sengupta, K., Sipila, M., Smith, J. N., Steiner, G., Tome, A., Virtanen, A., Wagner, A. C., Weingartner, E., Wimmer, D., Winkler, P. M., Ye, P. L., Carslaw, K. S., Curtius, J., Dommen, J., Kirkby, J., Kulmala, M., Riipinen, I., Worsnop, D. R., Donahue, N. M., and Baltensperger, U.: The role of low-volatility organic compounds in initial particle growth in the atmosphere, Nature, 533, 527-546, 2016.

Tunved, P., Strom, J., and Krejci, R.: Arctic aerosol life cycle: linking aerosol size distributions observed between 2000 and 2010 with air mass transport and precipitation at Zeppelin station, Ny-Alesund, Svalbard, Atmospheric Chemistry and Physics, 13, 3643-3660, 2013.

Twomey, S.: The Influence of Pollution on the Shortwave Albedo of Clouds, Journal of the Atmospheric Sciences, 34, 1149-1152, 1977.

von der Weiden, S. L., Drewnick, F., and Borrmann, S.: Particle Loss Calculator - a new software tool for the assessment of the performance of aerosol inlet systems, Atmospheric Measurement Techniques, 2, 479-494, 2009.

Wild, O., and Prather, M. J.: Global tropospheric ozone modeling: Quantifying errors due to grid resolution, Journal of Geophysical Research-Atmospheres, 111, D11305, 2006.

Willis, M. D., Burkart, J., Thomas, J. L., Kollner, F., Schneider, J., Bozem, H., Hoor, P. M., Aliabadi, A. A., Schulz, H., Herber, A. B., Leaitch, W. R., and Abbatt, J. P. D.: Growth of nucleation mode particles in the summertime Arctic: a case study, Atmospheric Chemistry and Physics, 16, 7663-7679, 2016.

Zhang, R. Y., Wang, L., Khalizov, A. F., Zhao, J., Zheng, J., McGraw, R. L., and Molina, L. T.: Formation of nanoparticles of blue haze enhanced by anthropogenic pollution, Proceedings of the National Academy of Sciences of the United States of America, 106, 17650-17654, 2009.

Ziemba, L. D., Dibb, J. E., Griffin, R. J., Huey, L. G., and Beckman, P.: Observations of particle growth at a remote, Arctic site, Atmospheric Environment, 44, 1649-1657, 2010.

Atmos. Chem. Phys. Discuss., https://doi.org/10.5194/acp-2018-428
Manuscript under review for journal Atmos. Chem. Phys.
Discussion started: 8 May 2018

Atmospheric Chemistry and Physics Discussions

Table 1. Particle growth rates for five growth events during the summers of 2015 and 2016.

Growth Event Number	Time period (UTC)				Growth rate (nm/h)
	Start		End		
GE 3 (Eureka)	2015-07-29	05:00	2015-07-30	11:00	0.420 ± 0.004
GE 3 (Alert)	2015-07-29	03:00	2015-07-30	12:00	0.50 ± 0.02
GE 6 (Eureka)	2015-08-02	04:00	2015-08-03	05:00	0.12 ± 0.08
GE 30 (Eureka)	2016-06-25	14:00	2016-06-27	20:00	1.01 ± 0.08
GE 32 (Eureka)	2016-07-04	05:00	2016-07-09	07:00	0.44 ± 0.01
GE 38 (Eureka)	2016-07-21	19:00	2016-07-25	19:00	0.352 ± 0.004

Atmos. Chem. Phys. Discuss., https://doi.org/10.5194/acp-2018-428
Manuscript under review for journal Atmos. Chem. Phys.
Discussion started: 8 May 2018

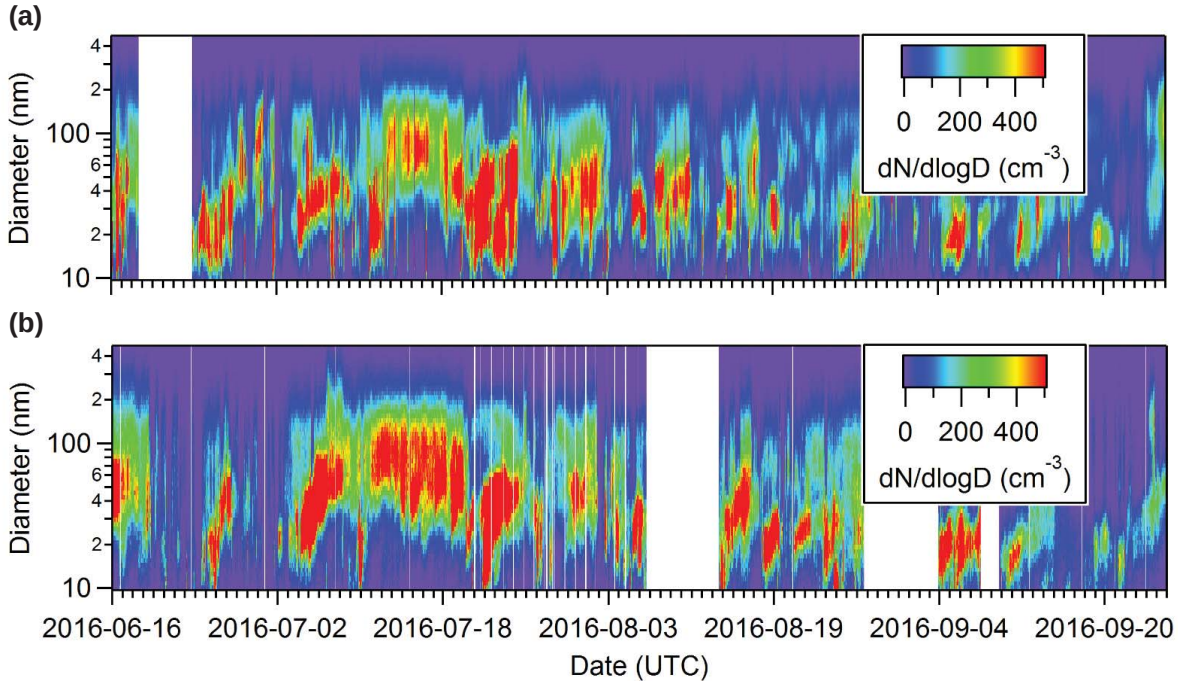

Fig 1. The size resolved particle concentration measured by SMPS instruments during summer 2016 in Alert **(a)** and at the PEARL RidgeLab **(b)** in the Canadian Arctic Archipelago.

Atmos. Chem. Phys. Discuss., https://doi.org/10.5194/acp-2018-428
Manuscript under review for journal Atmos. Chem. Phys.
Discussion started: 8 May 2018

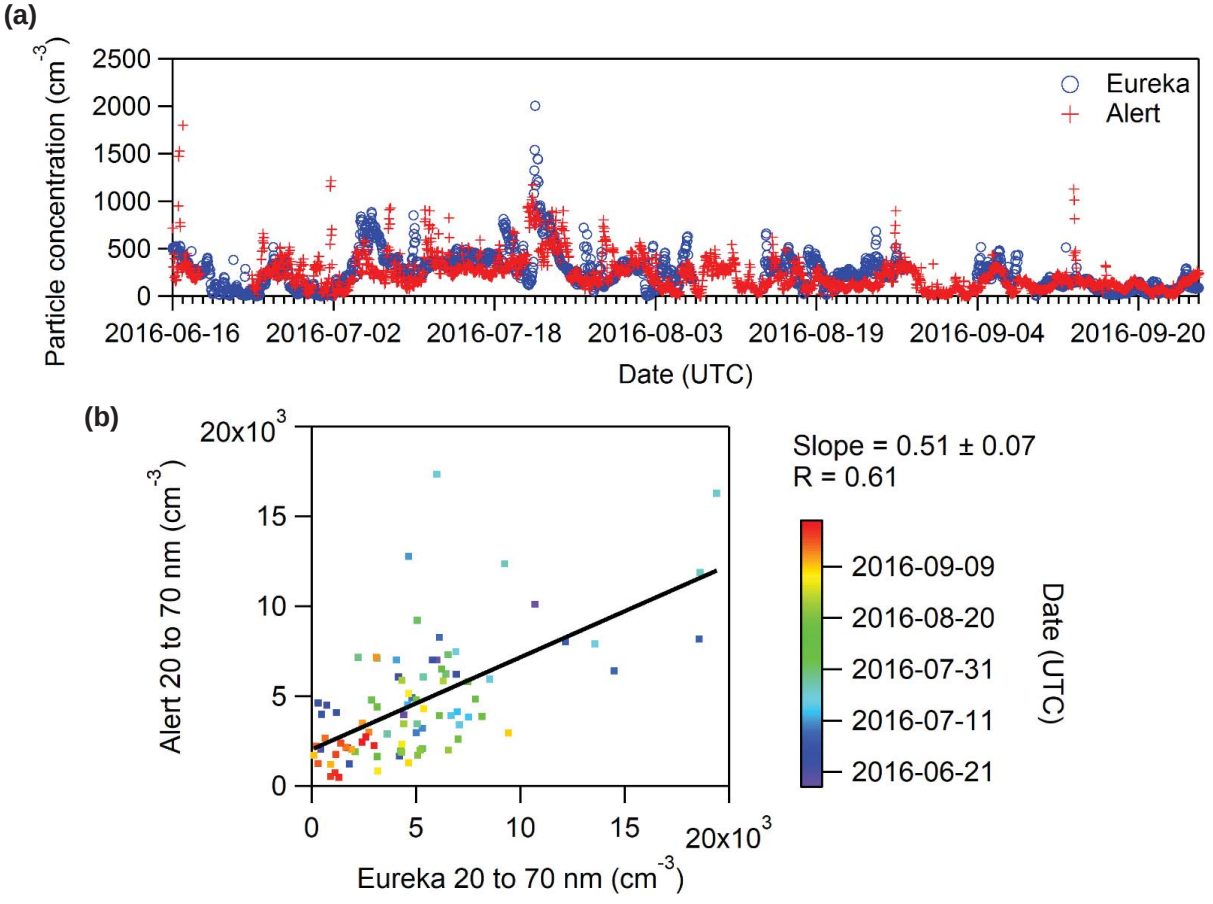

Fig 2. Total particle number concentrations measured at the PEARL RidgeLab near Eureka and in Alert during summer 2016 for sizes between 10 – 487 nm **(a)**. Scatter plot showing the correlation of the particle number concentrations measured in Alert and near Eureka **(b)**. The data in the scatter plot correspond to particle diameters between 20 and 70 nm.

Atmos. Chem. Phys. Discuss., https://doi.org/10.5194/acp-2018-428
Manuscript under review for journal Atmos. Chem. Phys.
Discussion started: 8 May 2018

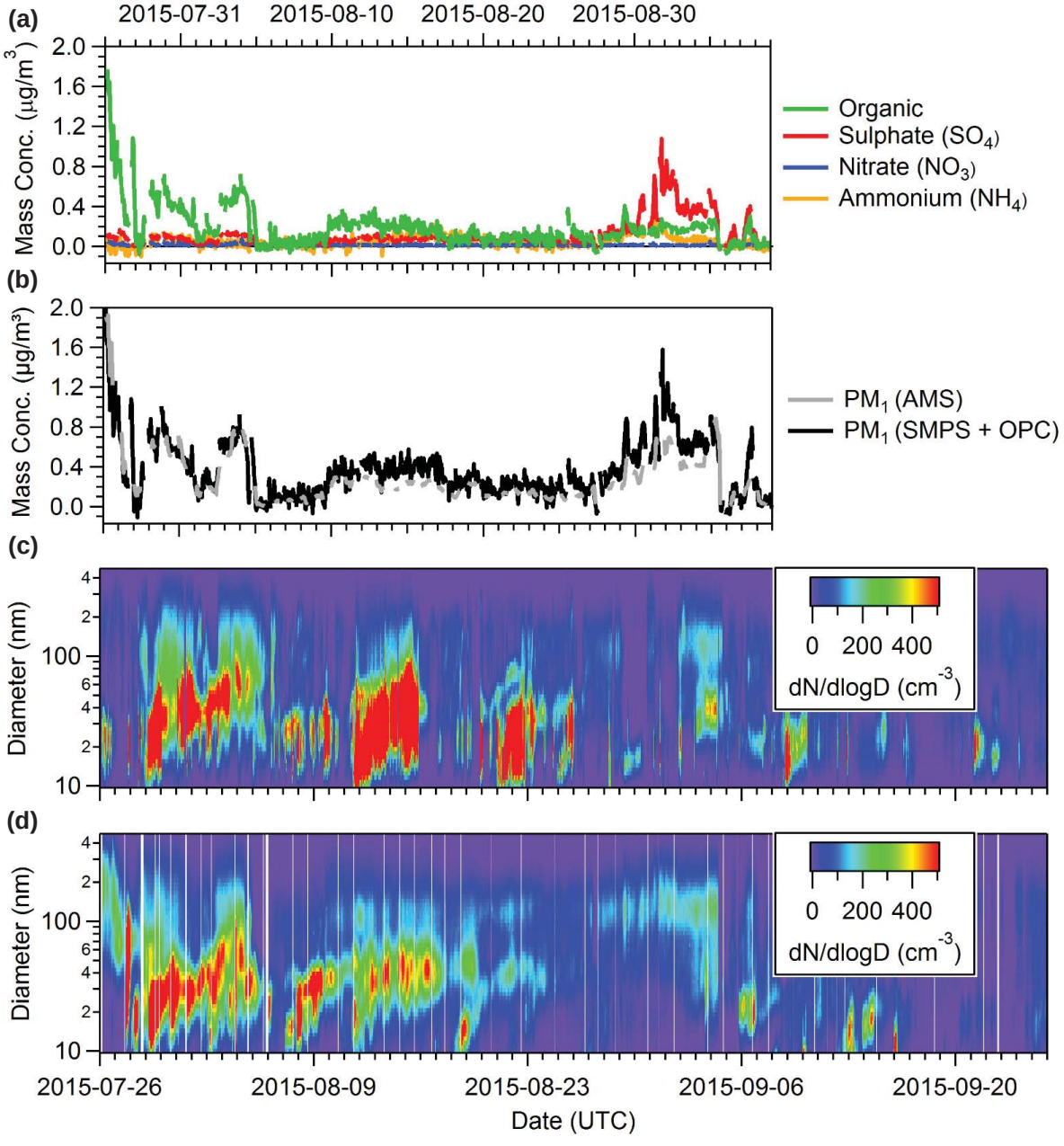

Fig 3. Aerosol mass spectrometry measurements of aerosol composition taken at the PEARL RidgeLab near Eureka **(a)**. The total concentration of non-refractory PM_1 aerosol measured by the mass spectrometer is also compared against the total PM_1 concentration measured by the SMPS and OPC, and exhibits good agreement with a linear regression analysis yielding a slope of 1.16 and a correlation coefficient of 0.89 **(b)**. In addition, the size resolved particle concentration measured by SMPS instruments during summer 2015 in Alert **(c)** and at the PEARL RidgeLab **(d)** are shown in the bottom two panels. All data are plotted on the same time scale.

Atmos. Chem. Phys. Discuss., https://doi.org/10.5194/acp-2018-428
Manuscript under review for journal Atmos. Chem. Phys.
Discussion started: 8 May 2018

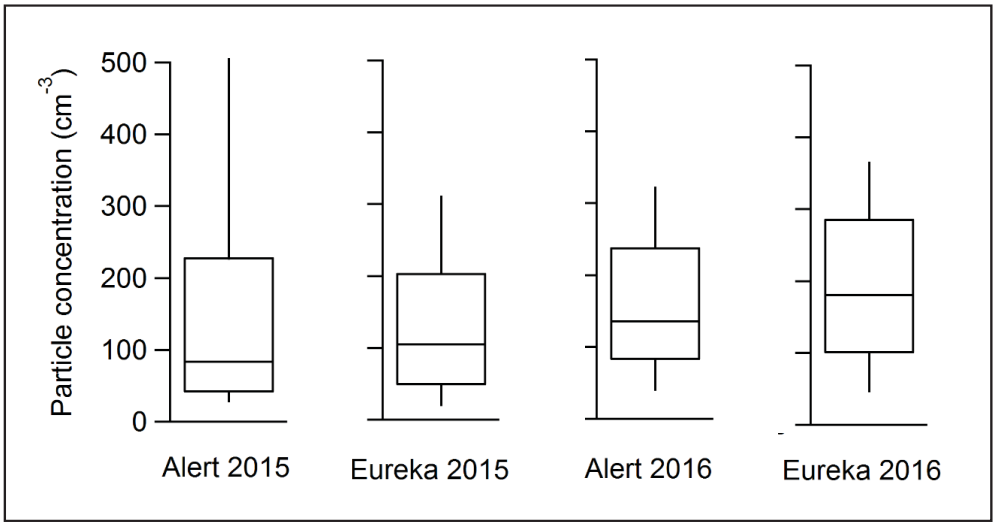

Fig 4. Box and whiskers plots of the total particle number concentrations (for diameters between 10 – 487 nm) measured during summer 2015 and during summer 2016 in Alert and at the PEARL RidgeLab near Eureka. The data plotted correspond to the period of 27 July to 9 September for both years. The plots indicate the 10th, 25th, 50th, 75th and 90th percentiles.

Atmos. Chem. Phys. Discuss., https://doi.org/10.5194/acp-2018-428
Manuscript under review for journal Atmos. Chem. Phys.
Discussion started: 8 May 2018

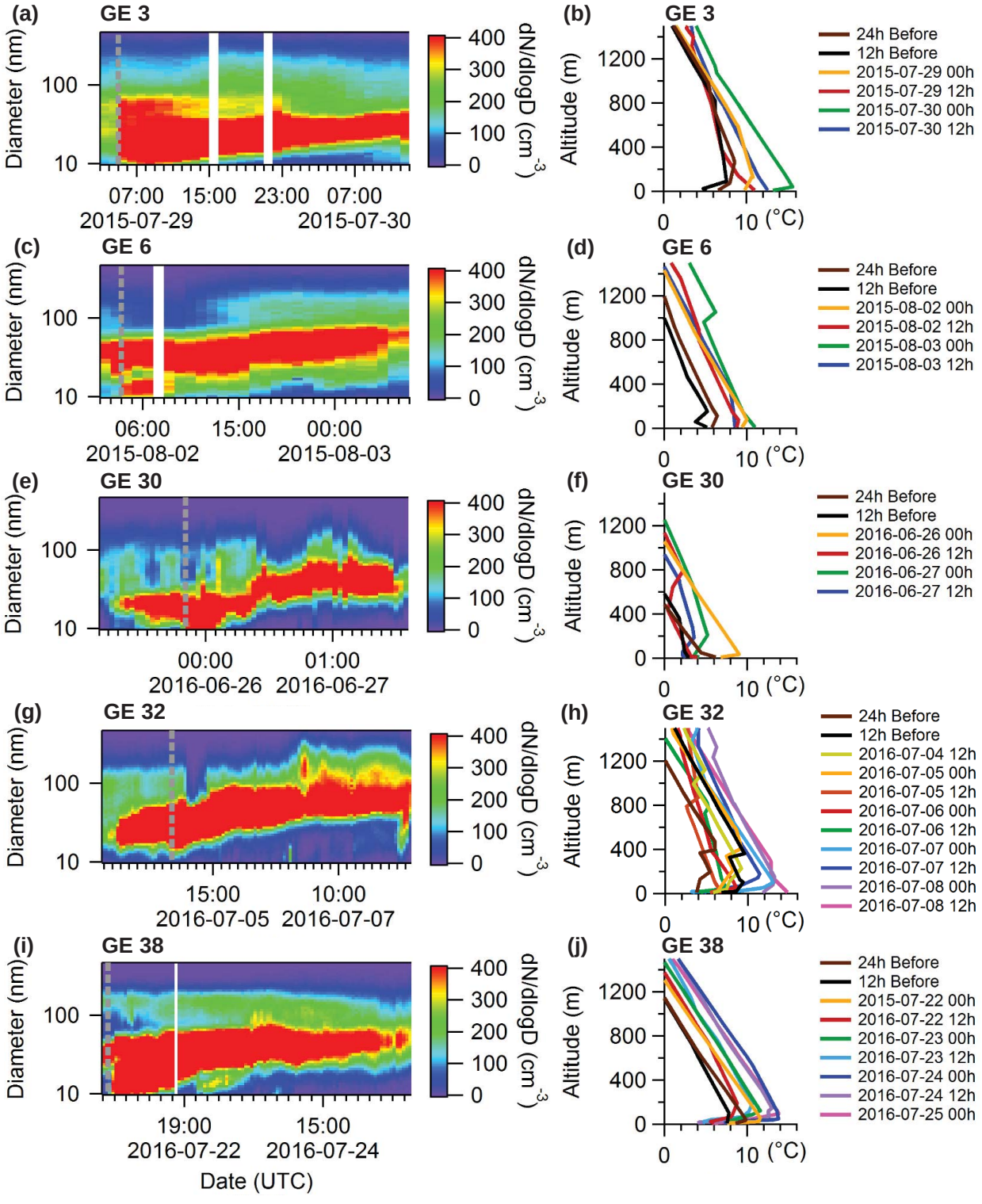

Fig 5. Five selected growth events near Eureka; the grey dashed line indicates the start of the growth event **(a, c, e, g, i)**. In the right column, vertical temperature profiles every 12h during the growth events are shown, including one day prior (24h) to the start of the growth event **(b, d, f, h, j)**.

Atmos. Chem. Phys. Discuss., https://doi.org/10.5194/acp-2018-428
Manuscript under review for journal Atmos. Chem. Phys.
Discussion started: 8 May 2018

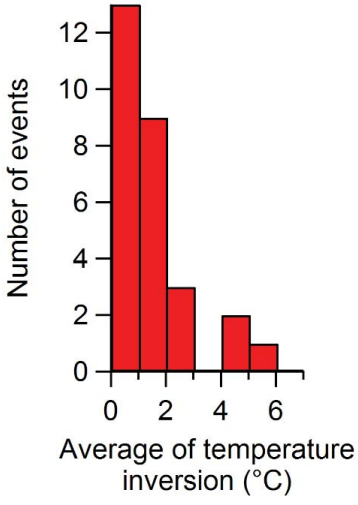

Fig 6. Histogram of the number of growth events near Eureka, binned by the average change in the temperature from 10 to 600 m above sea level. The average temperature change of each event is provided in Table S1, and is calculated from radiosonde measurements, as shown in Figure 5.

Atmos. Chem. Phys. Discuss., https://doi.org/10.5194/acp-2018-428
Manuscript under review for journal Atmos. Chem. Phys.
Discussion started: 8 May 2018

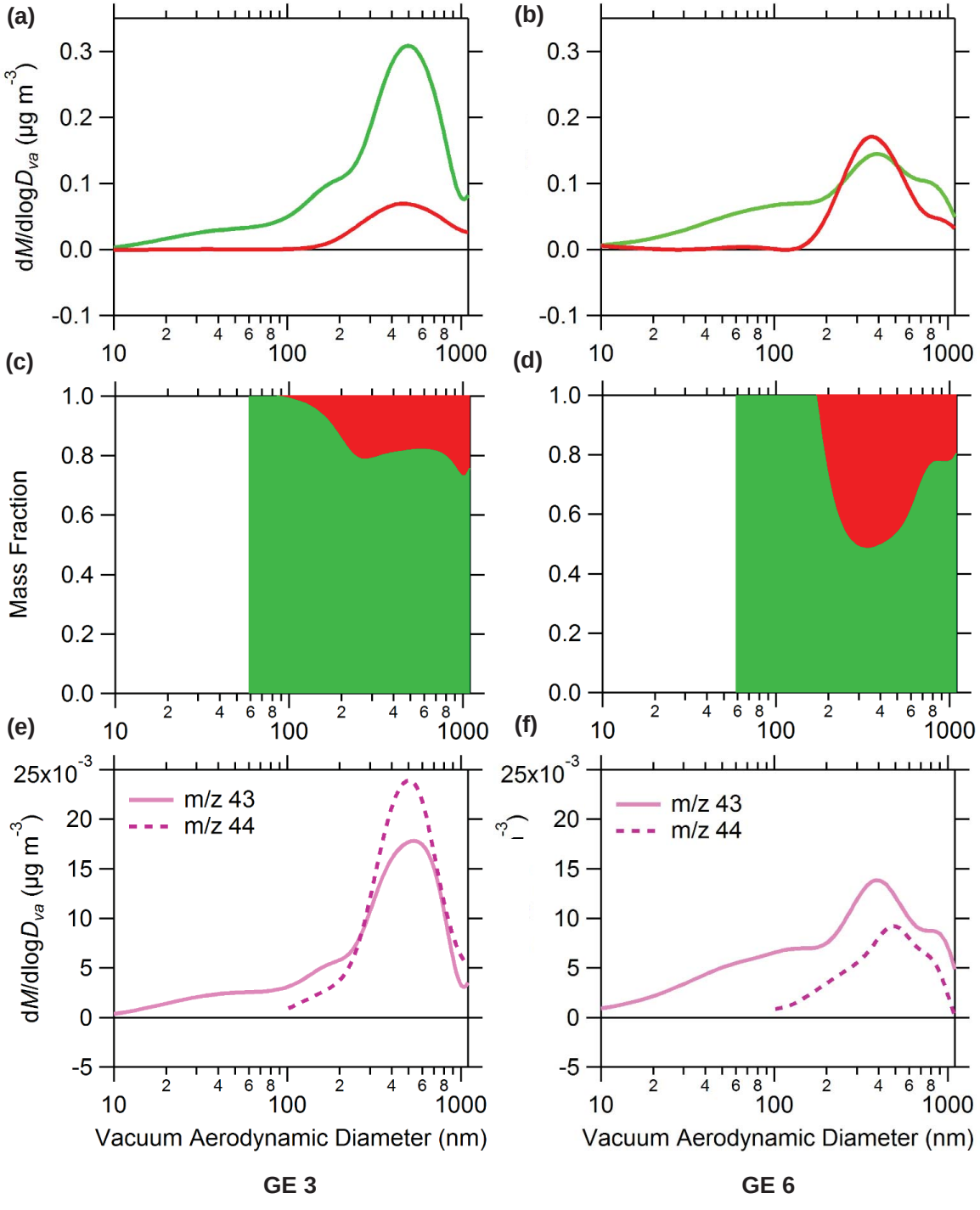

Fig 7. Size-resolved aerosol chemical composition for GE 3 **(a, c, e)** and GE 6 **(b, d, f)** measured near Eureka. The absolute organic and sulfate aerosol mass concentration **(a, b)**, the corresponding mass fractions **(c, d)**, and the nitrate-equivalent mass concentration of the m/z 43 and 44 fragments **(e, f)** are shown for each growth event. The data for m/z 44 is not shown below 100 nm due interference from gaseous CO_2.

Atmos. Chem. Phys. Discuss., https://doi.org/10.5194/acp-2018-428
Manuscript under review for journal Atmos. Chem. Phys.
Discussion started: 8 May 2018

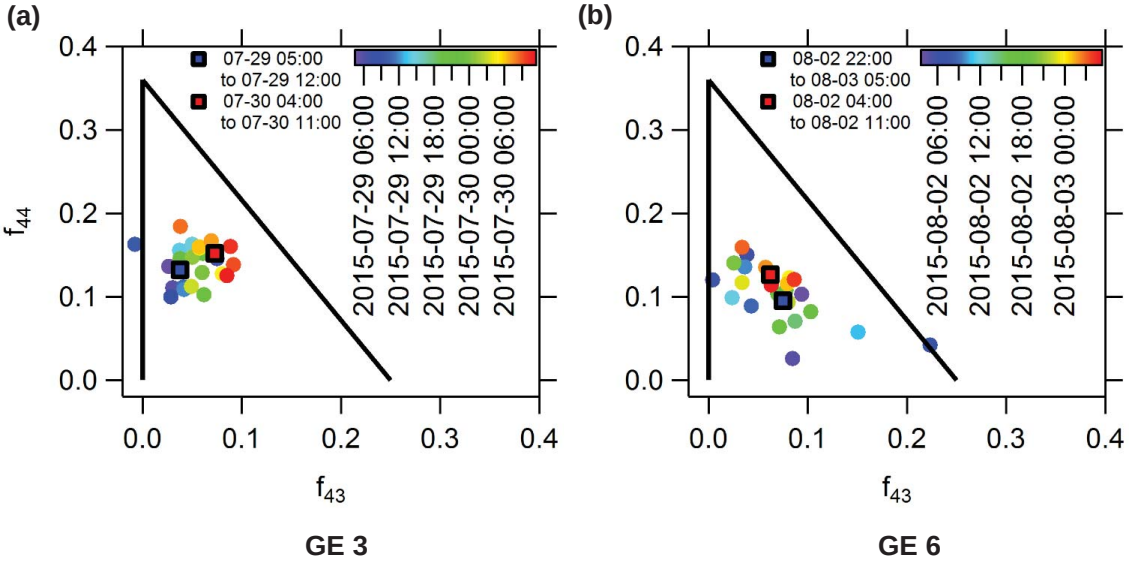

Fig 8. Scatter plot of the organic aerosol fraction measured at m/z 43 versus that measured at m/z 44 during GE 3 **(a)** and GE 6 **(b)** near Eureka. Also shown are the average values corresponding to the first seven and final seven hours of the growth event.